https://doi.org/10.1016/j.ymssp.2021.108120 **This is the Pre-Published Version.**

The following publication Qian, J., & Dong, Y. (2022). Uncertainty and multi-criteria global sensitivity analysis of structural systems using acceleration algorithm and sparse polynomial chaos expansion. Mechanical Systems and Signal Processing, 163, 108120 is available at https://doi.org/10.1016/j.ymssp.2021.108120.

# Uncertainty and multi-criteria global sensitivity analysis of structural systems using sparse polynomial chaos expansion and acceleration algorithm

Jing Qian[1] and You Dong[2, *]

[1] Research Assistant and Ph.D. Student, The Hong Kong Polytechnic University, Department of Civil and Environmental Engineering, Hung Hom, Kowloon, Hong Kong, jingce.qian@connect.polyu.hk.

[2] Assistant Professor of Structural Engineering, The Hong Kong Polytechnic University, Department of Civil and Environmental Engineering, Hung Hom, Kowloon, Hong Kong, you.dong@polyu.edu.hk. *Corresponding Author.

**Abstract:**

Sparse polynomial chaos expansion (PCE) can be used to emulate the stochastic model output where the original model is computationally expensive. It is a powerful tool in efficient uncertainty quantification and global sensitivity analysis. Structural systems are usually associated with high dimensional and probabilistic input. The number of candidate basis functions increases significantly with input dimension, resulting in high computational burden for establishing sparse PCE. In this study, acceleration techniques are integrated to formulate an algorithm for efficient computation of sparse PCE (ASPCE). The integrated algorithm can improve efficiency of computational process compared with conventional greedy algorithm while ensuring the satisfying predictive performance. Once the sparse PCE model is obtained, the statistic moments, probability density function of stochastic output, and global sensitivity index could be computed efficiently. Traditional PCE based global sensitivity analysis only assesses the sensitivity on individual structural performance criterion. Assessing the global sensitivity considering multiple criteria is challenging as the sensitive parameters may not be consistent for different performance criteria. To address this issue, a two-stage multi-criteria global sensitivity analysis algorithm is proposed herein by coupling ASPCE and the technique for order preference by similarity to ideal solution (TOPSIS). A holistic global sensitivity index is proposed to identify the sensitive parameters incorporating multiple performance criteria. In order to illustrate the efficiency, accuracy, and applicability of the proposed approach, two illustrative cases are presented.

**Keywords:** Uncertainty quantification; multi-criteria global sensitivity analysis; structural systems; sparse polynomial chaos expansion; acceleration algorithm.

## 1. Introduction

The input parameters of modeling structural systems are associated with uncertainties resulting in stochastic output. Uncertainty quantification aims to assess the uncertainty propagation from input to output. The Monte Carlo simulation (MCS) is a commonly used approach for uncertainty quantification. However, the computational expense of MCS could become unaffordable if the computational time of the original model is high. The surrogate model, representing the complex relationship between the input and output, can be used to emulate the output of a model efficiently. The uncertainty quantification can be conducted efficiently by using surrogate models. The surrogate models have been used in several engineering applications. For instance, Ebad Sichani and Padgett [1] assessed the collision between vertical concrete dry casks using surrogate models, and the polynomial response surface with stepwise regression was found to be suitable among the investigated surrogate models. Mangalathu *et al*. [2] compared the performance of different regression techniques on bridge seismic demand modeling, and Lasso regression was found to be the most effective one in terms of mean square error and absolute error. Ghosh *et al.* [3] investigated four surrogate models, and the parameterized fragility models were developed by employing logistic regression. The artificial neural network and Bayesian approach were also considered as alternative surrogate models to facilitate structural performance assessment [4,5]. The PCE is another type of surrogate model, which has been applied to several engineering problems [6–8]. The PCE could be used to compute the random response with higher efficiency compared with MCS [9]. The applications of PCE on complex structural systems considering multiple performance criteria are still limited. Additionally, a systematic comparison of PCE with other types of surrogate models is seldom conducted for structural systems.

The PCE utilizes the spectral representation on an appropriately established basis of polynomial functions [10,11]. The number of significant terms of PCE is relatively small due to the negligible high-order interaction effects and different effects of input variable on output [12]. Hence, the sparse PCE which only contains a small number of significant terms was

introduced. Under the same accuracy level, the required number of model evaluations for establishing sparse PCE is found to be smaller than full PCE, thus computational burden can be saved significantly by using sparse PCE [12]. Some greedy algorithms such as orthogonal matching pursuit (OMP) [13] and least-angle regression [14] were proposed to establish the sparse PCE. Additionally, algorithms were developed to establish sparse approximations using the techniques of reweighting coefficients [15] and adapting the dictionary of basis functions [16]. One challenging issue within the conventional greedy algorithms is the high computational burden for high dimension input problems. The number of candidate basis functions increases significantly with the input dimension, the computational cost of developing sparse PCE could increase subsequently, since a complete evaluation of the candidate set is needed to identify the appropriate basis functions at each iteration. The degree of polynomial could have significant influence on the system response, the computation cost is high for high degree cases, and acceleration algorithm is needed in such cases [17]. To address this issue in this paper, three techniques including probabilistic reduction of basis function candidates, QR decomposition, and early stopping criterion are combined to formulate an integrated acceleration algorithm for the computation of sparse PCE (ASPCE), and the computational burden of developing sparse PCE within high-dimensional engineering problems can be reduced. Specifically, the probabilistic reduction of basis function candidates is implemented. Instead of evaluating the whole candidate set, a subset of candidate basis functions is sampled and evaluated, thus the computational time can be reduced significantly and is independent with the input dimension and total degree of polynomials. Furthermore, to avoid the unnecessary iterations within the algorithm, the evolution of leave-one-out (LOO) error is investigated for structure systems, and the LOO error based early stopping criterion is proposed to further accelerate the computation.

Structural performance assessment is associated with uncertainties from different sources [18–20]. The sensitivity analysis could aid the rational treatment of uncertainties in modeling process. The sensitivity analysis can be categorized as local sensitivity analysis and global sensitivity analysis. The local sensitivity analysis reveals the local impact of input on the model

by computing the gradient of the response associated with its parameters around a nominal value [21]. The local sensitivity analysis can only provide the information at the point where local sensitivity is computed, the rest of the input space could not be explored [22]. The global sensitivity analysis aims to quantify the effects of the whole variations of input variables on the output. Compared with local sensitivity analysis, the global sensitivity analysis could avoid the limited exploration of the input space and take the interaction of different factors into consideration [22]. The global sensitivity analysis is preferred, when the model is associated with nonlinearity, large level of uncertainty, and interactions among input parameters [23]. It is worth noting that the global sensitivity index is based on the decomposition of variance. It uses the information of output variance without the full information of probability density function of the output. Additionally, it only reflects the amplitude of the global sensitivity without the direction of influence of the input variable. It may not be applicable when the sensitivity information from other aspects is concerned. Decision makers could choose different sensitivity analysis approaches based on the information of interest. This study focuses on the global sensitivity analysis. The Monte Carlo methods were developed in [24] to compute the global sensitivity index. In this approach, running a large number of the physical models is needed, and the computational time is high especially for complex structural systems. Then, Sudret [21] derived the sensitivity index using the coefficients of the PCE. Once the PCE model is established, the PCE based global sensitivity index can be computed analytically by post-processing the PCE coefficients with negligible computational cost. For a structural system, the responses associated with multiple performance criteria are of interest, the developed sensitivity analysis can only identify the sensitive parameters on individual structural performance criterion. The critical parameters could be different considering different structural performance criteria [5]. Based on traditional global sensitivity analysis, it is challenging to identify the sensitive parameters considering all performance objectives. To address this issue, a two-stage multi-criteria global sensitivity analysis algorithm is proposed in this paper. The global sensitivity indices are first computed for the response associated with individual performance criterion. Then, holistic global sensitivity indices are computed by

employing the technique for order preference by similarity to ideal solution (TOPSIS) [25]. The proposed holistic global sensitivity index incorporates the trade-off among the responses of multiple performances and serves as a holistic measure. The ranking of the sensitive parameters considering multiple structural performance criteria could be determined by the proposed holistic global sensitivity index.

To sum up, there exists extensive computational burden associated with developing sparse PCE for high dimension engineering systems. Previous applications regarding sparse PCE mainly focus on relatively simple structures and loading scenarios. It is necessary to further investigate the performance and applicability of the acceleration algorithm and sparse PCE within other complex engineering systems. Additionally, there is not a PCE based sensitivity analysis approach which could be adopted directly for assessing the global sensitivity incorporating multiple structural performance criteria. These issues are addressed in this study. The early stopping criterion, probabilistic reduction of basis function candidates, and QR decomposition are integrated to formulate an acceleration algorithm for solving high dimension engineering problems. Furthermore, a two-stage multi-criteria global sensitivity analysis algorithm is proposed by coupling the PCE based global sensitivity analysis with TOPSIS. The holistic global sensitivity considering multiple structural performance criteria could be assessed comprehensively. The developed approaches are illustrated on two examples. To the best knowledge of the authors, this is the first time to implement sparse PCE from acceleration algorithm to assess the vulnerability of multi-responses highway bridges under earthquake hazards. The performance of sparse PCE and acceleration algorithm for this engineering problem is investigated. These applications and investigations can provide new implications for uncertainty quantification of highway bridges subjected to natural hazards.

A schematic diagram illustrating the ASPCE for uncertainty quantification and global sensitivity analysis is presented in Figure 1. The probabilistic distributions of the input variables are identified. Through the experimental design, a set of input samples can be generated, and the corresponding outputs are computed by physical models. Then, the developed acceleration algorithm is performed to establish the sparse PCE model using the

training data. The global sensitivity, statistic moments, and probability density function (PDF) of response can be efficiently computed. The uncertainty propagation from the input to output is accomplished through the ASPCE.

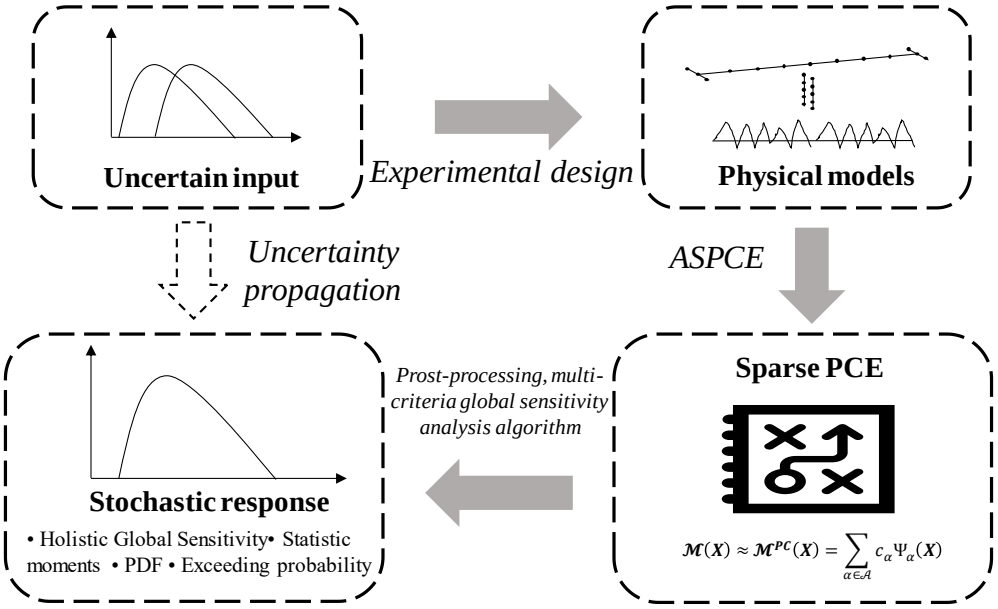


**Figure 1**. Illustration of uncertainty quantification and global sensitivity analysis using ASPCE

Overall, this paper formulates an acceleration algorithm for the computation of sparse PCE. The uncertainty quantification and global sensitivity analysis could be accomplished efficiently using the established sparse PCE. A two-stage multi-criteria global sensitivity analysis algorithm is proposed for holistic global sensitivity assessment considering multiple structural performance criteria. Two case studies with increasing complexity are conducted to illustrate the accuracy and efficiency of the proposed approach. In the first case, the approach is applied to a frame structure and the results are verified by MCS. Then, the proposed approach is applied to more complex structures to assess the structural probabilistic performance and holistic global sensitivity index. The remainder of this paper is organized as follows. The concepts of PCE are introduced in section 2. A conventionally greedy algorithm for establishing sparse PCE is presented in section 3. The ASPCE is illustrated in Section 4. The proposed two-stage multi-criteria global sensitivity analysis algorithm is introduced in Section 5. Two

illustrative examples are presented in Section 6. Section 7 contains summary and conclusions.

## 2. Polynomial chaos expansion (PCE)

Let $\boldsymbol{\mathcal{M}}$ represent a computational model. The random input vector $\boldsymbol{X} \in \mathbb{R}^M$ of $\boldsymbol{\mathcal{M}}$ is described by a joint PDF $\boldsymbol{f_X}$. The response of the system $Y = \boldsymbol{\mathcal{M}}(\boldsymbol{X})$ has a finite variance, the PCE of $\boldsymbol{\mathcal{M}}(\boldsymbol{X})$ is expressed as follows [11]

$$Y = \boldsymbol{\mathcal{M}}(\boldsymbol{X}) = \sum_{\alpha \in \mathbb{N}^M} c_\alpha \Psi_\alpha(\boldsymbol{X}) \tag{1}$$

where $\Psi_\alpha(\boldsymbol{X})$ are the multivariate polynomials orthonormal with respect to $\boldsymbol{f_X}$; $\alpha \in \mathbb{N}^M$ is a set of indices mapping to the components of the $\Psi_\alpha(\boldsymbol{X})$; and $c_\alpha$ are the coefficients.

The multivariate polynomials are computed as

$$\Psi_\alpha(\mathbf{x}) = \prod_{i=1}^{M} \phi_{\alpha_i}^{(i)}(x_i) \tag{2}$$

where $\phi_{\alpha_i}^{(i)}$ is the univariate orthogonal polynomial with respect to the $i^{th}$ variable in degree $\alpha_i$.

For practical purposes, original PCE is truncated to a finite sum and the truncated PCE is

$$\boldsymbol{\mathcal{M}^{PC}}(\boldsymbol{X}) = \sum_{\alpha \in \mathcal{A}} c_\alpha \Psi_\alpha(\boldsymbol{X}) \tag{3}$$

where $\mathcal{A}$ is the truncated set of multi-indices of multivariate polynomials. The PCE is truncated by setting the total degree of all the polynomials associated with the input variables smaller than or equal to $p$ as [26]

$$\mathcal{A}^{M,p} = \{\alpha \in \mathbb{N}^M : |\alpha| \leq p\}, card\mathcal{A}^{M,p} \equiv P = \frac{(p+M)!}{p!M!} \tag{4}$$

After the truncation, the coefficients can be computed using the least square solution as follows [23,27]

$$\widehat{\boldsymbol{C}} = (\boldsymbol{\Phi}^T\boldsymbol{\Phi})^{-1}\boldsymbol{\Phi}^T\boldsymbol{Y}, \quad \boldsymbol{\Phi} = \begin{pmatrix} \Psi_0(\mathbf{x}^{(1)}) & \cdots & \Psi_{card\mathcal{A}^{M,p}-1}(\mathbf{x}^{(1)}) \\ \vdots & \ddots & \vdots \\ \Psi_0(\mathbf{x}^{(N)}) & \cdots & \Psi_{card\mathcal{A}^{M,p}-1}(\mathbf{x}^{(N)}) \end{pmatrix} \tag{5}$$

where $\widehat{\boldsymbol{C}}$ is the computed vector of coefficients; $\boldsymbol{Y}$ is the vector of the model evaluations at *N* input vectors $\mathbf{x}^{(1)}, \ldots, \mathbf{x}^{(N)}$; and $\Psi_i(.), i = 0, \ldots, card\mathcal{A}^{M,P} - 1$ are the basis functions.

Once the PCE is obtained, it could be used to compute the uncertainty features (e.g., PDF and statistic moments) of the output efficiently [28]. The sparse PCE models which exclude the insignificant terms perform better in some studies [12] and are introduced in the following section.

## 3. Orthogonal matching pursuit for sparse PCE

Doostan and Owhadi [13] presented a greedy algorithm orthogonal matching pursuit (OMP) for establishing sparse PCE. The OMP sequentially selects the basis functions and adds them to the approximation from the candidate set. For each iteration, the OMP selects a basis function which is most correlated with the residual from a dictionary set by solving [29]

$$h(k) = \text{argmax}_{i \in \mathbb{C}_k} \frac{|\langle \boldsymbol{\psi}_i, \mathbf{r}_{k-1} \rangle|}{\|\boldsymbol{\psi}_i\|_2} \tag{6}$$

where $\Psi_{h(k)}$ is the selected basis function at iteration *k*; $\mathbb{C}_k$ is the updated dictionary at iteration *k* by excluding the basis function selected at iteration *k* – 1; $\boldsymbol{\psi}_i$ represent the evaluations using basis function *i*; and $\mathbf{r}_{k-1}$ represents the residual from the PCE associated with iteration *k* – 1.

At each iteration, the coefficients for currently selected basis functions are computed based on least square regression. The residual $\mathbf{r}_{k-1}$ is given by

$$\mathbf{r}_{k-1} = \boldsymbol{\Phi}_{k-1}\boldsymbol{C}_{k-1} - \boldsymbol{Y} \tag{7}$$

where $\boldsymbol{\Phi}_{k-1}$ is the matrix containing the evaluations using the basis functions at iteration *k* – 1 and $\boldsymbol{C}_{k-1}$ are the coefficients obtained at iteration *k* – 1.

The selection procedures are repeated and stopped until $\|\mathbf{r}\|_2$ is below the tolerance. This tolerance is predetermined through *v*-fold cross-validation technique.

## 4. Acceleration algorithm for computation of sparse PCE (ASPCE)

To avoid the high computational burden associated with the conventional greedy algorithms for computation of sparse PCE, three techniques are utilized within the acceleration algorithm and are introduced as follows.

*Technique 1: Probabilistic reduction of basis function candidates*

A lemma presented by Smola and Schölkopf [30] is applied herein to reduce the computational burden. Instead of selecting the basis functions from the full dictionary, it is possible to select the basis functions from the subsets of dictionary with satisfying performance. Let $\delta_1, \ldots, \delta_{ns}$ represent *ns* independent variables which follow identical distribution. The cumulative distribution function (CDF) of them is expressed as

$$\mathbb{p}(\delta_i \leq \tau) = F(\tau) \tag{8}$$

The CDF of $\delta := max_{i\in[ns]}\delta_i$ is expressed as

$$\mathbb{p}(\delta \leq \tau) = (F(\tau))^{ns} \tag{9}$$

Based on $\delta_i := (\boldsymbol{\psi}_i^T \mathbf{r}_k)^2 / \|\boldsymbol{\psi}_i\|_2^2$, by evaluating *ns* basis functions, the selection process at one iteration can guarantee a basis function within top $(1 - F(\tau)) \times 100\%$ of the full candidate set with probability $\vartheta$. The number of evaluated basis functions is computed as

$$ns = \frac{log(1-\vartheta)}{log\ F(\tau)} \tag{10}$$

*Technique 2: QR decomposition and efficient updating*

The QR factorization based approach for solving the coefficients could satisfy efficiency requirement and is more numerically stable. The $\boldsymbol{\Phi}_k \in \mathbb{D}^{N\times k}$ is decomposed as

$$\boldsymbol{\Phi}_k = \mathbf{QR}, \mathbf{Q} \in \mathbb{D}^{N\times k}, \mathbf{R} \in \mathbb{D}^{k\times k} \tag{11}$$

where $\mathbb{D}^{N\times k}$ represents the dimension of the matrix is $N \times k$; and $\mathbb{D}^{k\times k}$ represents the dimension of the matrix is $k \times k$.

After performing a new iteration, a new basis function is selected and the Gram-Schmidt process with re-orthogonalization [31] is used to update the QR factorization. Then, the coefficients of the PCE associated with current iteration are computed by solving

$$\mathbf{R}_k \boldsymbol{C}_k = (\mathbf{Q}_k)^T \boldsymbol{Y} \tag{12}$$

The conventional method for computing the residual requires to solve the PCE coefficients. By using the QR factorization, the residual can be updated efficiently without computing the coefficients as [32]

$$\mathbf{r}_k = \mathbf{r}_{k-1} - (\mathbf{Q}_k(:,k))^T \boldsymbol{Y} \mathbf{Q}_k(:,k) \tag{13}$$

*Technique 3: Implementation of early stopping criterion*

The trade-off between the complexity of the surrogate model and the number of experimental design points should be considered [7]. By training a small number of points to obtain a complex sparse PCE model (e.g., a large number of basis functions), the error of sparse PCE model using these trained points could be small. However, it may have large errors for the unseen data (e.g., generated new input data points). In this way, the surrogate model is over-fitted.

To avoid the over-fitting problem, the LOO cross-validation is used for model selection. The LOO error is computed as follows [12]

$$e_{\boldsymbol{X}}\left[\boldsymbol{\mathcal{M}}_{\boldsymbol{X},S}\right] = \frac{1}{N}\sum_{i=1}^{N}\left(\boldsymbol{\mathcal{M}}\left(\mathbf{x}^{(i)}\right) - \boldsymbol{\mathcal{M}}_{\boldsymbol{X}\setminus i,S}\left(\mathbf{x}^{(i)}\right)\right)^2 \tag{14}$$

where $e_{\boldsymbol{X}}\left[\boldsymbol{\mathcal{M}}_{\boldsymbol{X},S}\right]$ is the LOO error; $\boldsymbol{X} = \mathbf{x}^{(1)}, \ldots, \mathbf{x}^{(N)}$ represent $N$ realizations of input vectors; $\boldsymbol{\mathcal{M}}_{\boldsymbol{X},S}$ is the surrogate model $S$ established using data set $\boldsymbol{X}$; $\boldsymbol{\mathcal{M}}\left(\mathbf{x}^{(i)}\right)$ is the evaluation at the input vector $\mathbf{x}^{(i)}$; $\boldsymbol{\mathcal{M}}_{\boldsymbol{X}\setminus i,S}$ is the surrogate model $S$ trained by leaving the $i^{\text{th}}$ data out of $\boldsymbol{X}$; and $N$ is the number of samples.

For the PCE based methods, it is not necessary to train $N$ PCE models to compute the LOO error, alternatively, the LOO can be computed with one analysis as [12]

$$e_{\mathcal{X}}\left[\mathcal{M}_{\mathcal{X},S}\right] = \frac{1}{N}\sum_{i=1}^{N}\left(\frac{\mathcal{M}(\mathbf{x}^{(i)}) - \mathcal{M}_{\mathcal{X},S}(\mathbf{x}^{(i)})}{1-h_i}\right)^2 \quad (15)$$

where $h_i$ is the $i$th term of the $diag(\boldsymbol{\Phi}(\boldsymbol{\Phi}^T\boldsymbol{\Phi})^{-1}\boldsymbol{\Phi}^T)$.

The LOO error can also be expressed as residual error as [33]

$$e_{\mathcal{X}}\left[\mathcal{M}_{\mathcal{X},S,k}\right] = \frac{1}{N}\sum_{i=1}^{N}\left(\frac{\mathbf{r}_{k,i}}{\partial \mathbf{r}_{k,i}/\partial \boldsymbol{Y}_i}\right)^2 \quad (16)$$

Based on QR decomposition, the LOO error can be rewritten as [32]

$$e_{\mathcal{X}}\left[\mathcal{M}_{\mathcal{X},S,k}\right] = \frac{1}{N}\sum_{i=1}^{N}\left(\frac{\mathbf{r}_{k,i}}{\mathbf{1}-\mathbf{Q}_k(\boldsymbol{i},:)\mathbf{Q}_k(\boldsymbol{i},:)^T}\right)^2 \quad (17)$$

As illustrated, the LOO error can be efficiently computed through the QR decomposition at each iteration. The LOO error can be adopted as a model selection criterion to overcome the over-fitting problem. Traditionally, a greedy algorithm can be used to perform all possible iterations and the LOO errors are recorded at each iteration. The sparse PCE model associated with the minimum LOO error is chosen as the final model. In this study, the evolution of LOO error from iterations is investigated in case study parts. To avoid unnecessary iterations, the LOO error based criterion for early stopping the algorithm is proposed.

Overall, this study focuses on reducing the computational time of developing sparse PCE within high-dimensional engineering problems, by combining the three acceleration techniques: probabilistic reduction of basis function candidates; efficient updating using QR decomposition; and implementation of early stopping criterion. The three techniques accelerate the algorithm from different aspects, and each technique interacts with others. For instance, the leave-one-out error-based early stopping criterion is used to speed up the algorithm by avoiding unnecessary iterations, and QR decomposition is used to reduce the burden of computing this early stopping criterion. Within basis function selection, reduction of basis function candidates is adopted to reduce the computational burden, the residual, which is used in basis function selection, can be efficiently updated by QR decomposition. Each of the three techniques interacts with others to jointly reduce the computational burden.

The computational process of the integrated ASPCE is illustrated in Table 1. The evolution

of LOO error from iterations is investigated, and the LOO error based criterion for stopping the algorithm is proposed. At each iteration, a subset of basis function candidates is sampled from the whole dictionary. From the subset candidates, the algorithm finds the basis function which is most correlated with the current model residual, and the identified basis function is then added to the active set. The residual and LOO error are updated using currently selected basis functions based on QR decomposition. These procedures are repeated, and the algorithm is stopped once meeting the stopping criterion. The coefficients of the sparse PCE are finally solved after stopping the iteration and the sparse PCE is established.

Table 1. Procedures of ASPCE

| Acceleration algorithm for computation of sparse PCE |
|---|
| 1. Initialization: determine the number of basis candidates in a subset; $\mathbb{C}_1 = \mathbb{C}$; $\mathbb{S}_0 = \emptyset$; $\mathbf{r}_0 = \boldsymbol{Y}$; $k = 1$. |
| 2. While: stopping criterion is not satisfied. |
| 3. Probabilistic sampling of subset basis candidates $\mathbb{C}_s \subseteq \mathbb{C}_k$. |
| 4. Find basis function $\Psi_{h(k)}$, so that $h(k) = \mathrm{argmax}_{i \in \mathbb{C}_s} \frac{\lvert\langle \boldsymbol{\psi_i}, \mathbf{r}_{k-1} \rangle\rvert}{\lVert \boldsymbol{\psi_i} \rVert_2}$. |
| 5. Remove selected basis from candidate set $\mathbb{C}_{k+1} = \mathbb{C}_k \backslash h(k)$. |
| 6. Add selected basis to active set $\mathbb{S}_k = \mathbb{S}_{k-1} \cup h(k)$. |
| 7. Compute residual $\mathbf{r}_k$ using QR decomposition. |
| 8. Update LOO error. |
| 9. $k = k+1$. |
| 10. End. |
| 11. Compute coefficients of PCE by solving $\mathbf{R}_m \boldsymbol{C} = (\mathbf{Q}_m)^{\boldsymbol{T}} \boldsymbol{Y}$. |

## 5. Novel two-stage multi-criteria global sensitivity analysis based on ASPCE and TOPSIS

### *5.1. Global sensitivity analysis for individual output parameter*

The contribution of uncertain input variables to the output variance can be quantified using global sensitivity analysis [21]. Traditionally, the global sensitivity index is computed by MCS with high computational cost especially for some complex models. By post-processing the PCE coefficients, the global sensitivity index can be computed efficiently. Let $\mathcal{H}_{i_1,\ldots,i_s}$ represent the

set from $\alpha \in \mathcal{A}$ where only the indices $\{i_1, \ldots, i_s\}$ are non-zero, the $\mathcal{H}_{i_1,\ldots,i_s}$ is expressed as

$$\mathcal{H}_{i_1,\ldots,i_s} = \{\alpha \in \mathcal{A}: \alpha_v = 0 \Leftrightarrow v \notin (i_1, \ldots, i_s), \forall\, v = 1, \ldots, M\} \tag{18}$$

The PCE based sensitivity indices are derived as [27]

$$S^{\mathcal{A}}_{i_1,\ldots,i_s} = \frac{\sum_{\alpha \in \mathcal{H}_{i_1,\ldots,i_s}} {c_\alpha}^2}{D_{\mathcal{A}}},\ D_{\mathcal{A}} = \sum_{\alpha \in \mathcal{A}\setminus\{0\}} {c_\alpha}^2 \tag{19}$$

The total sensitivity indices are computed as

$$S^{T,\mathcal{A}}_i = S^{\mathcal{A}}_i + \sum_{j<i} S^{\mathcal{A}}_{j,i} + \sum_{j<k<i} S^{\mathcal{A}}_{j,k,i} + \cdots + S^{\mathcal{A}}_{1,\ldots,M} \tag{20}$$

The Eq. (20) can be rewritten as

$$S^{T,\mathcal{A}}_i = \frac{\sum_{\alpha \in \mathcal{g}_i} {c_\alpha}^2}{D_{\mathcal{A}}} \tag{21}$$

$$\mathcal{g}_i = \{\alpha \in \mathbb{N}^M: 0 \leq |\alpha| \leq p, \alpha_{\,i} \neq 0\} \tag{22}$$

*5.2. Holistic global sensitivity analysis*

The conventional global sensitivity analysis reveals the effects of the input variable on one single output parameter. When multiple output parameters existing in a system are of interest, determining the overall sensitivity of the input with respect to multiple output parameters becomes a problem. In this study, the global sensitivity indices associated with different performance criteria are incorporated to compute the holistic global sensitivity index. The TOPSIS [25], a multi-criteria decision making technique, is extended herein to compute the holistic global sensitivity index. In this way, the overall sensitivity of input parameters considering multiple criteria could be assessed. The following part introduces the basic procedures of computing the holistic global sensitivity index. The global sensitivity indices associated with all the output parameters are formulated in a sensitivity index matrix **S** as

$$\mathbf{S} = \begin{pmatrix} S_{11} & \cdots & S_{1n_c} \\ \vdots & \ddots & \vdots \\ S_{n_i 1} & \cdots & S_{n_i n_c} \end{pmatrix} \tag{23}$$

where $S_{ij}$ is the global sensitivity index of the $i^{th}$ input parameter with respect to the $j^{th}$

performance criterion; $n_c$ is the number of performance criteria; and $n_i$ is the number of input parameters. The global sensitivity index used in Eq. (23) could be first-order or total order. The total order global sensitivity index describes the contribution of an input parameter to output variance considering the effects of its interaction with other input parameters [27,34]. The choice of first-order or total order depends on the concerns and requirements of the decision makers. If the decision makers desire the information including the interaction among different variables, the total order global sensitivity index can be chosen. If the isolated impact of the input variable is of concern, the first-order global sensitivity index can be chosen. If total global sensitivity index is used in Eq. (23), the interaction effects among different variables are incorporated in the decision making process.

Then, the sensitivity index matrix is normalized as

$$\bar{\mathbf{S}} = \begin{pmatrix} \bar{S}_{11} & \cdots & \bar{S}_{1n_c} \\ \vdots & \ddots & \vdots \\ \bar{S}_{n_i 1} & \cdots & \bar{S}_{n_i n_c} \end{pmatrix}, \quad \bar{S}_{ij} = \frac{S_{ij}}{\sqrt{\sum_{k=1}^{n_i} S_{kj}^2}} \tag{24}$$

where $\bar{\mathbf{S}}$ is the normalized sensitivity index matrix.

Different performance criteria could result in different importance to the system safety. The different preferences of performance criteria should be incorporated within the holistic global sensitivity index by implementing weighting factor. The weighting factor associated with different performance criteria determined by the decision maker is applied to the normalized sensitivity index matrix as

$$\hat{\mathbf{S}} = \begin{pmatrix} \hat{S}_{11} & \cdots & \hat{S}_{1n_c} \\ \vdots & \ddots & \vdots \\ \hat{S}_{n_i 1} & \cdots & \hat{S}_{n_i n_c} \end{pmatrix}, \quad \hat{S}_{ij} = w_j \times \bar{S}_{ij} \tag{25}$$

where $\hat{\mathbf{S}}$ donates the weighted and normalized sensitivity index matrix and $w_j$ represents the weighting factor for the $j^{th}$ performance criterion.

The ideal sensitivity solution is obtained by extracting the maximum values of sensitivity

indices associated with all input parameters. The negative-ideal solution is obtained conversely. These two sensitivity solutions are expressed as

$$S^{+}=\left\{\hat{S}_{1+},...,\hat{S}_{n_c+}\right\}=\left\{(\max \hat{S}_{ij}), i=1,...,n_i,\ j\in J\right\} \tag{26}$$

$$S^{-}=\left\{\hat{S}_{1-},...,\hat{S}_{n_c-}\right\}=\left\{(\min \hat{S}_{ij}), i=1,...,n_i,\ j\in J\right\} \tag{27}$$

The distance of the sensitivity associated with each input variable to the ideal solution and negative-ideal solution can be calculated. The holistic global sensitivity index is computed based on the relative closeness as

$$hs_i=\frac{\sqrt{\sum_{j=1}^{n_c}(\hat{S}_{ij}-\hat{S}_{j-})^2}}{\sqrt{\sum_{j=1}^{n_c}(\hat{S}_{ij}-\hat{S}_{j+})^2}+\sqrt{\sum_{j=1}^{n_c}(\hat{S}_{ij}-\hat{S}_{j-})^2}} \tag{28}$$

where $hs_i$ is the holistic global sensitivity index for the input valuable $i$.

*5.3. Interpretation of multi-criteria global sensitivity analysis*

The problem can be formulated as a multi-criteria decision making problem when there exist the following conditions: several alternatives serve as the comparable components; multiple criteria are used to describe the status of each alternative; and multiple objectives need to be satisfied. By considering multiple conflicting criteria, there may not exist a solution that is satisfying over all criteria. A compromise solution incorporating the trade-off consideration among multiple conflicting criteria can be obtained by using multi-criteria decision making techniques [35].

For an engineering system consisting of multiple outputs, different outputs may be associated with different sensitive parameters. There may not exist one input that is most sensitive to all outputs. The trade-off among multiple outputs should be considered. In this regard, sensitivity ranking of inputs considering multiple outputs can be formulated as a compromise multi-criteria decision making problem. Each input is considered as an alternative. For each input, the global sensitivity indices with respect to multiple outputs can be quantified

and they are considered as multiple ranking criteria. The objective is to determine the sensitivity raking of inputs considering the global sensitivity indices with respect to multiple outputs. TOPSIS, a robust compromise decision making approach, is extended herein to solve this multi-criteria decision making problem.

The basic idea of TOPSIS is to rank the alternatives based on distance, where the preferential alternative should have a long distance to the negative-ideal solution and a short distance to the ideal solution. Herein, the negative-ideal solution and ideal solution are represented as the ideal insensitive solution and ideal sensitive solution, respectively. The global sensitivity index matrix is used as a decision matrix in this study. Specifically, Eq. (28) is used to compute relative closeness as the last step in TOPSIS, and the ranking of alternatives is determined based on this index [25,35]. The numerator in Eq. (28) represents the distance of an alternative to the negative-ideal solution, and the denominator in Eq. (28) represents the sum of the distance of an alternative to the negative-ideal solution and ideal solution [25,35]. A preferential alternative should have a large value of relative closeness computed in Eq. (28). In the decision making of ranking inputs, a sensitive input considering multiple outputs should have a large value of relative closeness (long distance to the ideal insensitive solution and short distance to the ideal sensitive solution). Therefore, the holistic global sensitivity index is proposed based on Eq. (28) in this study. The sensitivity ranking of input parameters considering multiple outputs can be determined based on the proposed holistic global sensitivity index. The proposed holistic global sensitivity index can be regarded as a holistic measure and utilized to identify the sensitive input parameters considering multiple performance criteria.

The value of holistic global sensitivity index depends on many factors such as the global sensitivity indices with respect to all outputs, the importance of different outputs, and the trade-off consideration. This expression shows one of the advantages of the proposed approach, the different importance of outputs and the trade-off can be flexibly considered within the sensitive parameter identification process in TOPSIS. In real engineering problems, different outputs could be associated with different considerations of importance, the importance of outputs

represented by weighting factors in TOPSIS can be determined by judgement among experts.

The holistic global sensitivity index can be used to aid the decision makers to refine the database (e.g., data acquisition, investigation, and complexity reduction) for confident regional risk assessment. For instance, more efforts and resources can be spent on collecting and investigating holistic sensitive parameters. This index can also be used for the screening of holistic sensitive parameters considering the trade-off among multiple outputs. Based on the proposed holistic global sensitivity index, the sensitive and insensitive input parameters considering the trade-off among multiple outputs can be identified. By constraining the number of considered sensitive parameters, the top holistic sensitive parameters can be selected based on holistic global sensitivity index. In another way, decision makers could also determine the threshold of holistic global sensitivity index based on their requirement, and the parameters associated with global sensitivity indices exceeding the threshold can be identified as holistic sensitive parameters.

Overall, the ASPCE and TOPSIS coupled two-stage multi-criteria global sensitivity analysis algorithm is proposed to incorporate multiple performance criteria. The global sensitivity is first assessed for individual performance criterion. The global sensitivity indices associated with different performance outputs are then considered as the sensitivity criteria and formulated as a sensitivity matrix. TOPSIS is used to incorporate these sensitivity criteria to compute the holistic global sensitivity indices. The detailed algorithm is illustrated in Table 2. Both the global sensitivity indices and holistic global sensitivity indices provide information for rational treatment of the uncertainty within input parameters.

Table 2. Procedures of two-stage multi-criteria global sensitivity analysis

| Two-stage multi-criteria global sensitivity analysis algorithm |
|---|
| *Stage 1: Global sensitivity analysis considering individual performance criterion* |
| Determine *ni* uncertain variables and corresponding probabilistic distributions. |
| Conduct experimental design. |
| for performance criterion number *cn* = 1:*nc* |
| Formulate sparse PCE model for performance criterion *cn* using ASPCE. |
| Computed global sensitivity indices of *ni* variables with respect to the performance criterion |

*cn* by post-processing the PCE coefficients.
End
*Stage 2: Holistic global sensitivity analysis considering multiple performance criteria*
Formulate sensitivity index matrix **S.**
Compote normalized sensitivity matrix **NS**.
Determine the weighting factors of all performance criteria.
Compote normalized and weighted sensitivity matrix **VS**.
Extract ideal and negative-deal sensitivity solutions.
Compute the holistic global sensitivity indices based on relative closeness

## 6. Illustrative examples

The proposed framework of uncertainty quantification and global sensitivity analysis using ASPCE is illustrated in Figure 2. The computational procedures consist of three parts: initiation of training data; establishment of sparse PCE model; and post-processing of sparse PCE model. In the first stage, probabilistic distributions of the input variables are identified. A set of input samples is generated based on the experimental design, and the output parameters are computed by running the physical models. The sparse PCE model is obtained after performing the ASPCE. The uncertainty quantification and global sensitivity analysis can be accomplished efficiently.

The random variable could be dependent in nature. The proposed approaches can be extended to incorporate dependence within both uncertainty quantification and multi-criteria global sensitivity analysis. For the uncertainty quantification, the ASPCE can be applied for dependent parameters by incorporating the method from [36]. The copula [37], a flexible tool for capturing nonlinear dependence characteristics, is used to model the dependence structure of multiple inputs. The Rosenblatt and inverse Rosenblatt transforms are computed, and the original inputs are transformed to independent components. Thus, the uncertainty quantification methods (e.g., ASPCE) used for independent variables can be applied to dependent inputs [36]. For the multi-criteria global sensitivity analysis, the proposed approach can also be applied for dependent parameters by incorporating the method from [38]. The covariance decomposition is used to develop the sensitivity index associated with both uncorrelated and correlated contributions. The dependence among multiple inputs is

characterized using a copula-based approach. Based on the developed PCE model, the sensitivity index considering dependence can be computed by integrating copula approach and covariance decomposition [38]. Then, the computed sensitivity indices incorporating dependence can be used to perform multi-criteria global sensitivity analysis.

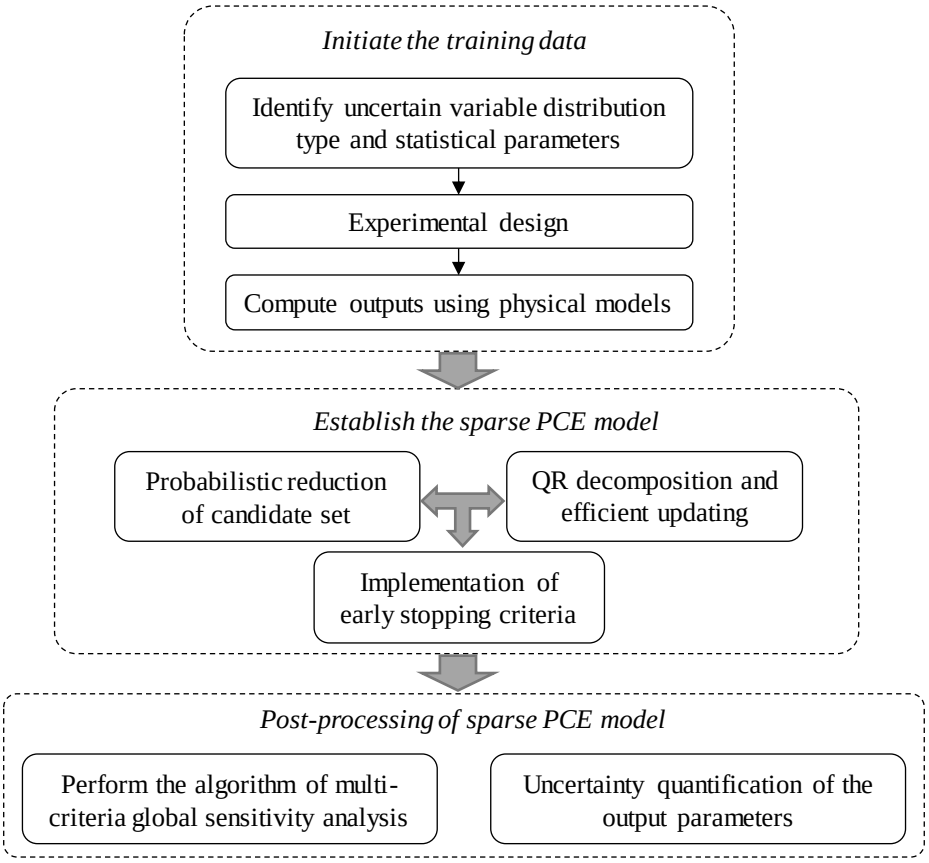


**Figure 2.** Framework of uncertainty quantification and global sensitivity analysis

In this section, the developed approach is applied to a frame structure firstly. Then, the presented framework is applied to a portfolio of bridges under seismic hazards. Within the investigated two examples, the performance of ASPCE is compared with OMP and other surrogate models: regression tree (RT), support vector machine (SVM), and Gaussian process regression (GPR). The basic ideas of these models are briefly introduced in this section.

The RT divides the data space into small sub-spaces and trains the models using each sub-space data. Since several data sub-spaces are produced by this approach, the interactions can be captured by the nonlinear model with several layers [39,40]. The SVM uses the kernels to convert the parameters into a high dimension space. The SVM model is expressed as the sum

of weighted nonlinear functions and a constant parameter. The selection of kernel and nonlinear functions are very important [1]. The GPR surrogate model is regarded as nonparametric kernel-based probabilistic models [41]. The GPR model describes the outputs by explicit basis functions and latent variables from a Gaussian process. The basis functions map the input parameters to high dimension space.

### *6.1. Case 1: Uncertainty quantification and global sensitivity analysis of a frame structure*

A three-span three-story frame structure under lateral loads is selected as the example. The sketch of the structure is illustrated in Figure 3, and the uncertain parameters considered are listed in Table 3. Three different lateral loads are applied to the left part of the structure. The displacement at the top right corner is considered as the response of interest.

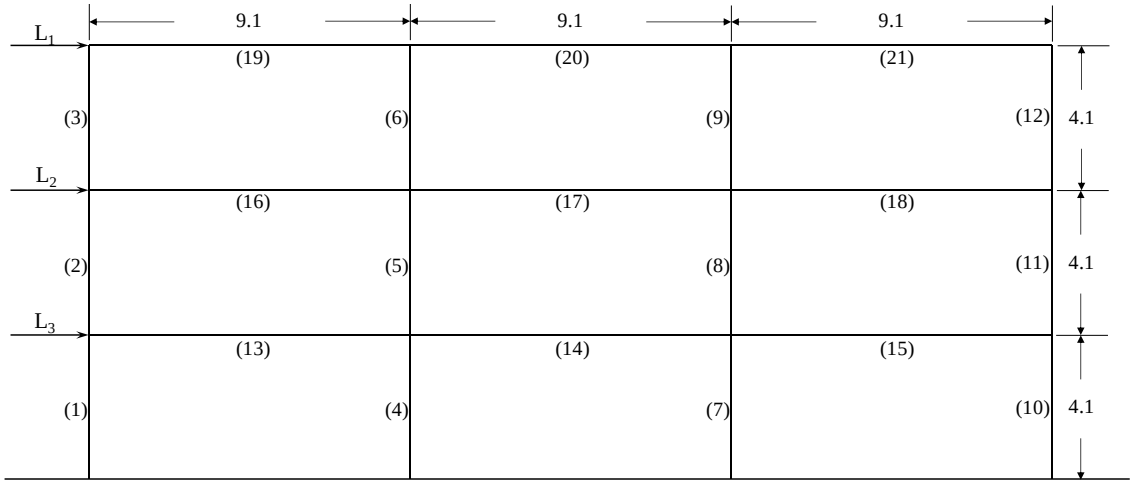


**Figure 3.** Investigated frame structure subjected to lateral loads (unit: m, the numbers indicate different elements and are mapped to the parameters in Table 3).

Table 3. Parameters used within the frame structure.

| Symbol | Parameter | Number | Units | Distribution type | $\mu$ | $\sigma$ |
|---|---|---|---|---|---|---|
| $L_1$ | Load 1 | 1 | N | Lognormal | $4.89 \times 10^5$ | $1.47\times 10^5$ |
| $L_2$ | Load 2 | 2 | N | Lognormal | $4\times 10^5$ | $1.6\times 10^5$ |
| $L_3$ | Load 3 | 3 | N | Lognormal | $2\times 10^5$ | $8\times 10^4$ |
| $E_{13\text{-}21}$ | Young's modulus (material property of elements 13-21) | 4 | $N/m^2$ | Lognormal | $1.98\times 10^{11}$ | $1.74\times 10^{10}$ |

| | | | | | | |
|---|---|---|---|---|---|---|
| $E_{1\text{-}12}$ | Young's modulus (material property of elements 1-12) | 5 | $N/m^2$ | Lognormal | $1.99\times 10^{11}$ | $1.75\times 10^{10}$ |
| $A_{1\text{-}3}$ | Cross-sectional area of elements 1-3 | 6 | $m^2$ | Lognormal | 0.0488 | 0.0087 |
| $A_{4\text{-}9}$ | Cross-sectional area of elements 4-9 | 7 | $m^2$ | Lognormal | 0.0590 | 0.0105 |
| $A_{10\text{-}12}$ | Cross-sectional area of elements 10-12 | 8 | $m^2$ | Lognormal | 0.0476 | 0.0085 |
| $A_{13\text{-}18}$ | Cross-sectional area of elements 13-18 | 9 | $m^2$ | Lognormal | 0.0224 | 0.004 |
| $A_{19\text{-}21}$ | Cross-sectional area of elements 19-21 | 10 | $m^2$ | Lognormal | 0.0130 | 0.0023 |
| $I_{1\text{-}3}$ | Moment of inertia of elements 1-3 | 11 | $m^4$ | Lognormal | 0.0014 | $1.86\times 10^{-4}$ |
| $I_{4\text{-}9}$ | Moment of inertia of elements 4-9 | 12 | $m^4$ | Lognormal | 0.0018 | $2.40\times 10^{-4}$ |
| $I_{10\text{-}12}$ | Moment of inertia of elements 10-12 | 13 | $m^4$ | Lognormal | 0.0015 | $2.00\times 10^{-4}$ |
| $I_{13\text{-}15}$ | Moment of inertia of elements 13-15 | 14 | $m^4$ | Lognormal | 0.0025 | $3.33\times 10^{-4}$ |
| $I_{16\text{-}18}$ | Moment of inertia of elements 16-18 | 15 | $m^4$ | Lognormal | 0.0021 | $2.80\times 10^{-4}$ |
| $I_{19\text{-}21}$ | Moment of inertia of elements 19-21 | 16 | $m^4$ | Lognormal | $7.617\times 10^{-4}$ | $1.01\times 10^{-4}$ |
| $M_f$ | Mass factor | 17 | - | Uniform | 1 | 0.058 |

Note: $\mu$ = mean value and $\sigma$ = standard deviation.

*Establishment of surrogate models*

The performance of surrogate models under different sample sizes is investigated. Based on the statistic parameters in Table 3, 8 sets of frame structure and load realizations (with sample sizes of 100, 200, 400, 600, 800, 1000, 1200, and 1400) are generated using Latin hypercube sampling technique [42]. The displacement at the top right corner can be computed using finite element model in OpenSEES. The 8 sets of input and output training data are obtained. As discussed previously, the LOO error is considered as the stopping criterion in ASPCE. In this study, the evolution of LOO error is investigated and an appropriate occasion for stopping the algorithm is proposed. The LOO errors changing with iterations are presented in Figure 4. The

results show that the evolution of LOO error is convex and smooth for the investigated case. To avoid the possible local minima of LOO error, the proposed early stopping criterion is to stop the algorithm when the LOO error continuously increases for ten iterations.

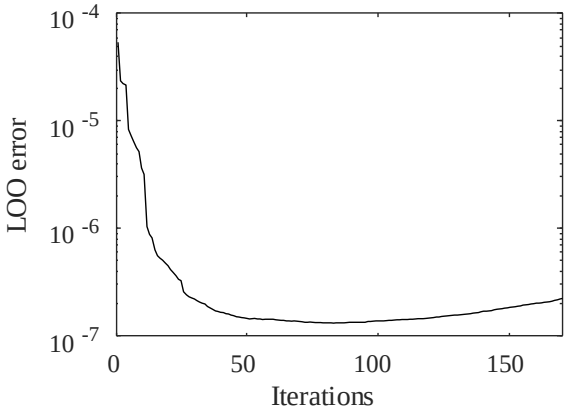


**Figure 4.** The evolution of the LOO error.

The surrogate models are trained using ASPCE, OMP, SVM, RT, and GPR under the 8 sets of training data. The training time of OMP and ASPCE is presented in Figure 5. The training time of OMP increases significantly with the total degree of polynomials while the training time of ASPCE is independent with the total degree of polynomials. The ASPCE seems to be more efficient than OMP under high total degree of polynomials. The superiority of ASPCE in terms of efficiency is further demonstrated in the following example.

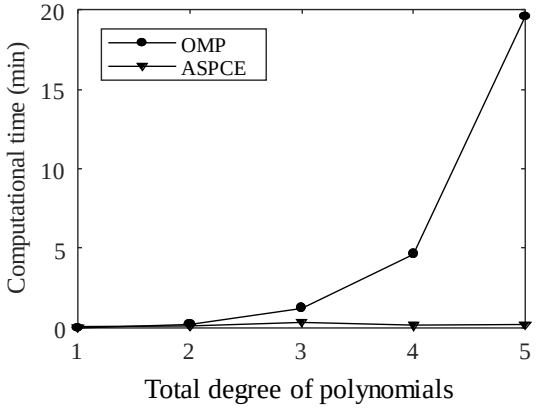


**Figure 5.** Training time of OMP and ASPCE associated with the investigated frame structure

*Validation of the surrogate models using Monte Carlo simulation (MCS)*

The brute-force MCS is used to validate the results obtained from surrogate models [43]. The

statistic moments, PDF, reliability indices, and global sensitivity indices computed from MCS serve as references to calculate the relative errors. Once the sparse PCE model is obtained, the statistic moments are computed analytically from the coefficients. The relative errors in mean and standard deviation of the five surrogate models under different sample sizes are presented in Figure 6. With respect to predictive performance in mean, the ASPCE, OMP, and GPR are identified as suitable surrogate models. The relative errors in mean from these three models converge after the sample size of 400 and maintain at relatively lower level after convergence. For the relative errors in standard deviation, the sparse PCE based methods ASPCE and OMP outperform other models under all sample sizes, while the GPR produces higher relative errors.

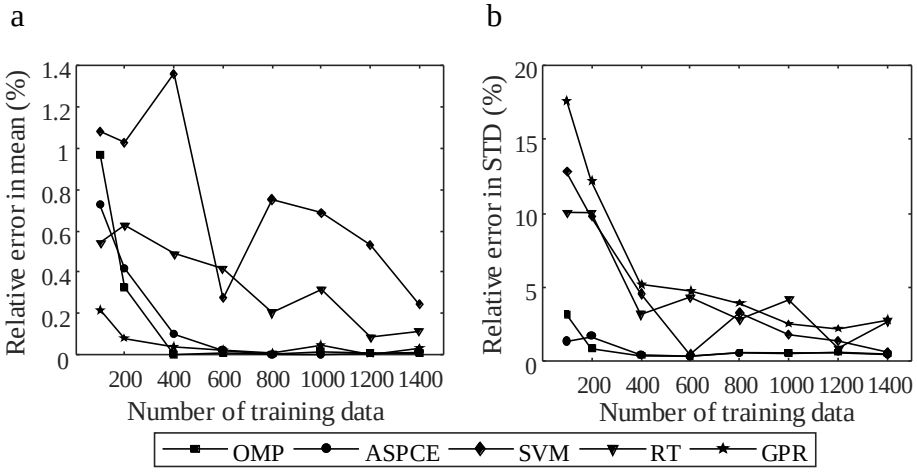


**Figure 6.** Relative errors in: (a) mean and (b) standard deviation under different sample sizes.

The relative errors in reliability indices for two different limit thresholds (e.g., 3 cm and 5 cm) are illustrated in Figure 7. For the case of limit threshold 3 cm, the errors from ASPCE, OMP, and GPR converge after the sample size of 200 and these three models stand out among the five. With respect to the limit threshold of 5 cm, the convergence sample size for ASPCE and OMP is 400. These two models have relatively lower errors than others in this scenario.

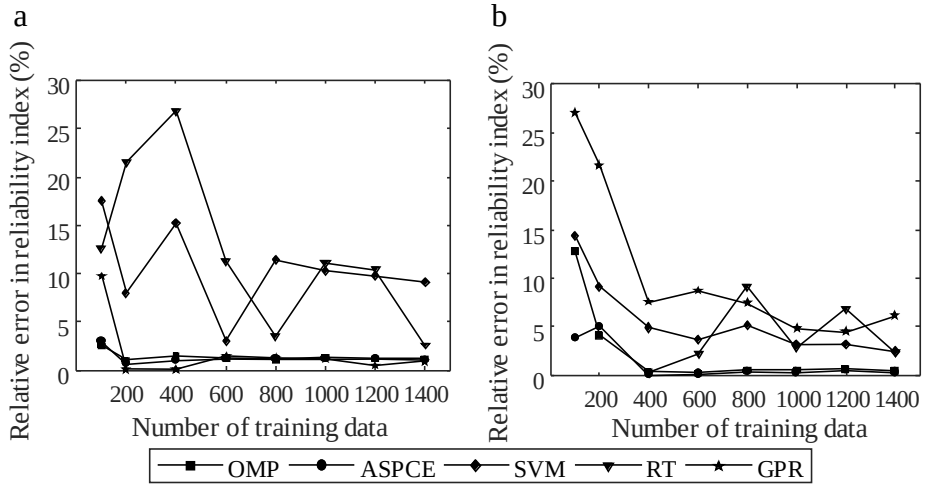


**Figure 7.** Relative errors of reliability indices under the limit thresholds of (a) 3 cm and (b) 5 cm, respectively.

The PDFs of the displacement obtained by ASPCE, GPR, and MCS are shown in Figure 8. The PDF from ASPCE matches perfectly with MCS. For the GPR, the errors can be observed around the peak and tail of PDF curve.

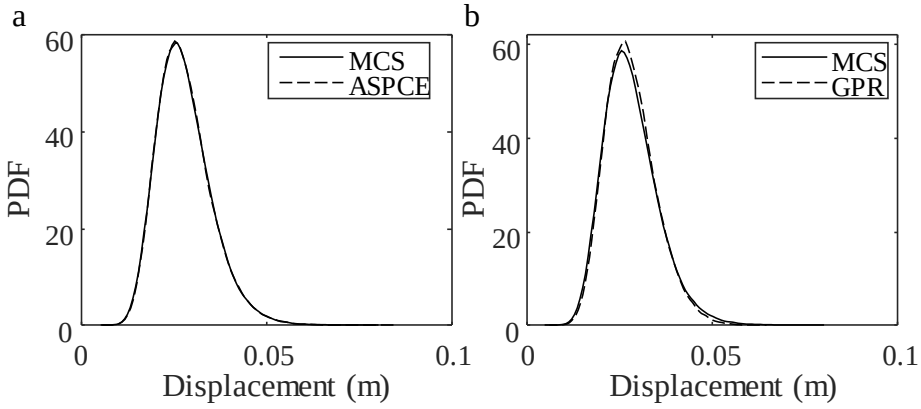


**Figure 8.** Comparisons of the PDFs computed by MCS and surrogate models of (a) ASPCE and (b) GPR.

Confidence interval provides the information on the confidence of estimated statistical results in consideration of the uncertainties [44]. The ASPCE derived 95% confidence intervals for mean of displacement, standard deviation of displacement, and reliability indices are presented in Table 4. The confidence intervals are narrow for the statistical moments and

reliability indices, indicating the computational confidence and stability of ASPCE.

Table 4. Confidence intervals of the results computed by ASPCE

| Confidence bounds | Mean | Standard deviation | Reliability index (limit threshold: 3 cm) | Reliability index (limit threshold: 5 cm) |
|---|---|---|---|---|
| Lower bound | $2.797\times10^{-2}$ | $7.346\times10^{-3}$ | 0.383 | 2.366 |
| Upper bound | $2.802\times10^{-2}$ | $7.413\times10^{-3}$ | 0.394 | 2.426 |

Note: the unit of displacement computed using ASPCE is m.

In addition to the uncertainty quantification, PCE can also aid efficient global sensitivity analysis. Instead of conducting time-consuming MCS in the traditional method, the global sensitivity indices can be computed analytically by post-processing the PCE coefficients. The results are compared with those from MCS in Figure 9. The results show that the ASPCE-derived sensitivity indices agree well with MCS-derived reference values.

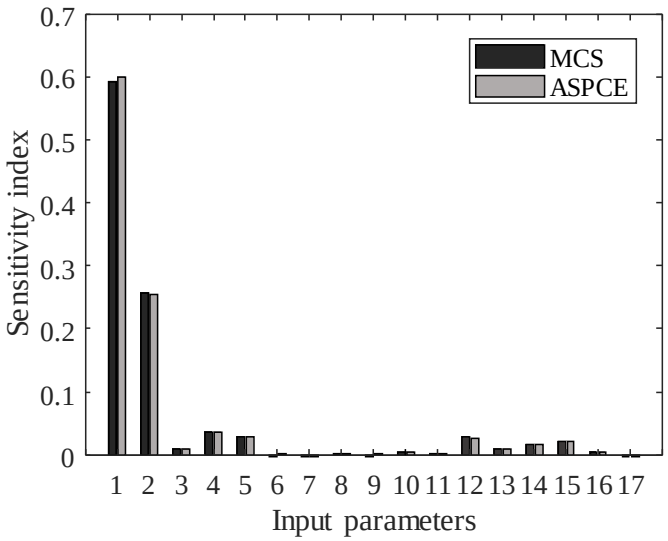


**Figure 9.** Sensitivity indices with respect to the frame displacement (the numbers on *x* axis represent different input parameters as indicated in Table 3)

The computational time of uncertainty quantification and sensitivity analysis can be saved significantly by using the ASPCE. In uncertainty quantification, the data from running 400 finite element models (FEMs) is used in ASPCE, while the data from running $10^5$ FEMs is used in MCS. With respect to sensitivity analysis, 400 finite element model evaluations are used in

ASPCE, while a total of $N_{MCS}(M+2) = 10^5 \times (17+2) = 1.9 \times 10^6$ finite element model evaluations are used in MCS for sensitivity analysis [45], where $N_{MCS}$ is the sample size of MCS. The total computational time of MCS and ASPCE is presented in Table 5.

Table 5. Total computational time of different methods

| | MCS | ASPCE |
|---|---|---|
| Computational time of reliability | 6 h | 2 min |
| Computational time of sensitivity | 116 h | 2 min |

To sum up, the sparse PCE based methods ASPCE and OMP outperform among the investigated surrogate models in terms of uncertainty quantification accuracy, and ASPCE provides accurate estimation of global sensitivity indices. The training time of ASPCE is less compared with OMP under high degree cases. By using ASPCE, the total time of uncertainty quantification and sensitivity analysis could be reduced significantly compared with conventional MCS, in the meanwhile, this method provides satisfying accuracy.

### *6.2. Case 2: Multi-criteria global sensitivity analysis of bridges under earthquakes*

In this case, the seismic demand surrogate models are obtained after performing the training algorithm. The performance of different surrogate models (e.g., ASPCE, OMP, SVM, RT, and GPR) is compared. The multi-criteria global sensitivity analysis is performed for the bridges. The seismic fragility using the information from multi-criteria global sensitivity analysis is computed.

A class of continuous RC bridges is selected as the investigated bridges. In regional risk assessment, the bridges distributed within a region could have different material and geometric parameters. Conventionally, it is impractical to develop the fragility curves for each specific structure in a region, as the computational time is extensive. Developing bridge class level fragility, by incorporating material and geometric uncertainties within a class, can be one possible solution to address this challenge [46]. The bridge class level fragility is used to describe the damage probabilities for the bridges within a class under earthquakes. To facilitate the regional risk assessment, the bridge class level fragility should be developed and

incorporate the uncertainties from hazards, material and geometric parameters [2,46]. Thus, the uncertainties associated with material and geometric parameters should be considered in training of surrogate model [5]. The probabilistic parameters of these bridges are summarized in Table 6. Based on the probabilistic distributions of the bridge parameters, the bridge realizations are sampled using Latin hypercube sampling technique [42]. The finite element models of the bridge realizations are established using the software OpenSEES [47–49]. The finite element model of the bridge is shown in Figure 10. For each bridge sample, one ground motion from [50] is randomly selected and coupled with this bridge sample. So that the input data including bridge samples and ground motions are obtained. The number of the ground motions and that of the Latin hypercube sampling structures are identical. The ground motions used for coupling with bridge samples are associated with different intensities and characteristics. Thus, these input samples incorporate the uncertainties associated with bridge geometry, material, and ground motions. A set of nonlinear time history analyses using the input samples is performed to obtain the training data. The seismic demands of different components can be computed using the developed finite element model [51,52].

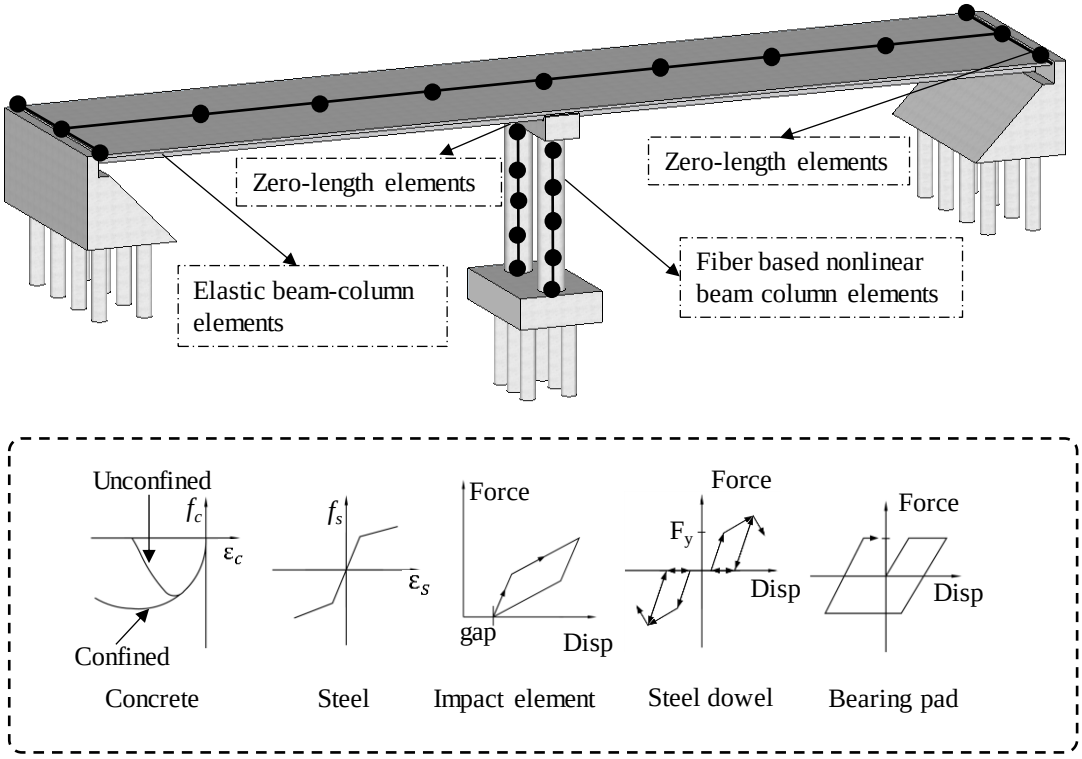


**Figure 10.** Finite element model of the bridge

Table 6. Parameters used within the bridges

| Parameters | Number | Units | Distribution type | $\mu$ | $\sigma$ | Ref. |
|---|---|---|---|---|---|---|
| Concrete compressive strength | 1 | MPa | Normal | 29.03 | 3.59 | [2] |
| Reinforcing steel yield strength | 2 | MPa | Lognormal | 465.0 | 37.30 | [2] |
| Span length | 3 | mm | Lognormal | 31775 | 8738 | [2] |
| Deck width | 4 | mm | Lognormal | 11970 | 2418 | [2] |
| Column height | 5 | mm | Lognormal | 6625 | 865 | [2] |
| Abutment backwall height | 6 | mm | Lognormal | 2186 | 441 | [2] |
| Bearing coefficient of friction | 7 | - | Normal | 0.3 | 0.1 | [2] |
| Strength of a composite of two dowels | 8 | kN | Lognormal | 116 | 9.28 | [53] |
| Abutment-deck gap | 9 | mm | Lognormal | 23.5 | 12.5 | [2] |
| Backfill initial stiffness at the benchmark backwall height | 10 | N/m/cm | Lognormal | 384 | 138 | [54] |
| Backfill ultimate capacity at the benchmark backwall height | 11 | kN/m | Lognormal | 475 | 111 | [54] |
| Damping | 12 | | Normal | 0.045 | 0.0125 | [2] |
| Foundation translational spring stiffnesses | 13 | N/mm | normal | 140101 | 105076 | [2] |
| Shear modulus of elastomeric pad | 14 | MPa | Uniform | 1.365 | 0.407 | [53] |
| Mass factor | 15 | - | Uniform | 1 | 0.058 | [53] |
| Longitudinal reinforcement ratio | 16 | (%) | Uniform | 2.25 | 0.52 | [2] |

Note: $\mu$ = mean value and $\sigma$ = standard deviation.

*Performance of surrogate models*

The training for the surrogate model is carried out once using the data consisting of ground motions with different intensities, structure samples, and seismic demands from finite element models. The uncertainties associated with structures and ground motions are considered in uncertainty quantification. To further testify the applicability of the proposed LOO error based

stopping criterion, the evolution of LOO error is investigated in this case. To the authors' best knowledge, the evolution of LOO error on bridge seismic demands has not been investigated in previous studies. The results show that the evolution of LOO error of ASPCE is convex and smooth, and proposed LOO error based stopping criterion is still applicable.

The predictive performance of surrogate model can be evaluated in terms of the mean squared error (MSE) on an independent test sample set [4]. The MSEs of the investigated models on a test sample set are computed and listed in Figure 11. The effects of the training sample sizes on predictive performance are also investigated. As indicated, the sparse PCE based methods (e.g., ASPCE and OMP) outperform other models for all considered sample sizes. The ASPCE provides similar predictive performance with OMP.

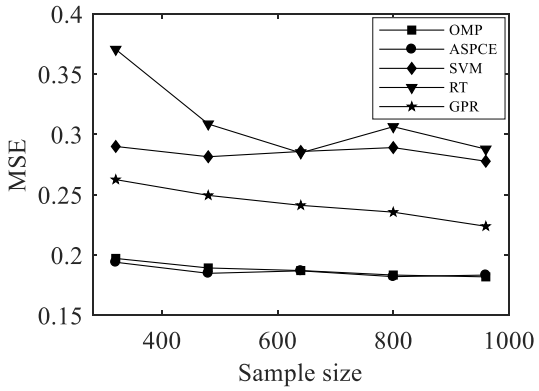


**Figure 11.** MSE of the seismic demands on a test sample set under different training sample sizes

The training time for each model is calculated as the sum of the training time for all the structural components. The training time for two sparse PCE based methods with increasing total degree of polynomials is illustrated in Figure 12. The training time of OMP increases significantly with total degree of polynomials, while the training time of ASPCE is negligible and independent with total degree of polynomials. The improved efficiency of the ASPCE can be interpreted through the three speeding-up techniques. As illustrated in Figure 13, the number of candidate basis functions increases significantly with total degree of polynomials and input dimensions. With the implementation of probabilistic reduction of basis function candidates, the ASPCE would evaluate a subset of polynomial candidates, while the OMP uses the whole

dictionary. Additionally, the number of evaluated candidates is constant at all degrees and input dimensions in ASPCE. This consistency ensures the training time of ASPCE is independent with the total degree of polynomials and input dimensions. This speeding-up technique ensures that the ASPCE can be performed for high degree and high dimension problems with negligible computational cost. With the implementation of QR decomposition, the residual and LOO error can be efficiently updated at each iteration without solving the PCE coefficients, while the OMP relies on solving the coefficients at each iteration. The implementation of stopping criteria aids the ASPCE to avoid unnecessary iterations and early stop at an appropriate occasion. The stopping of OMP needs the determination of an optimal error tolerance which is computed by cross-validation, and this process induces additional computational time.

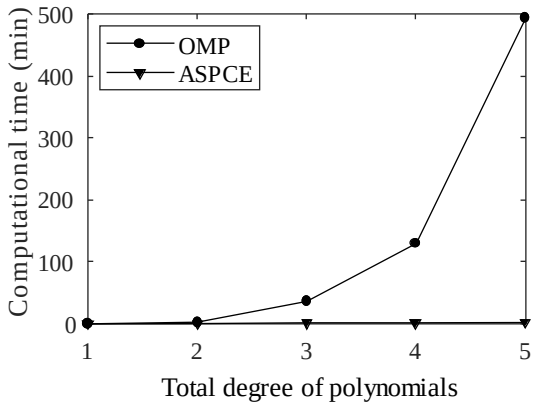


**Figure 12.** Training time of OMP and ASPCE

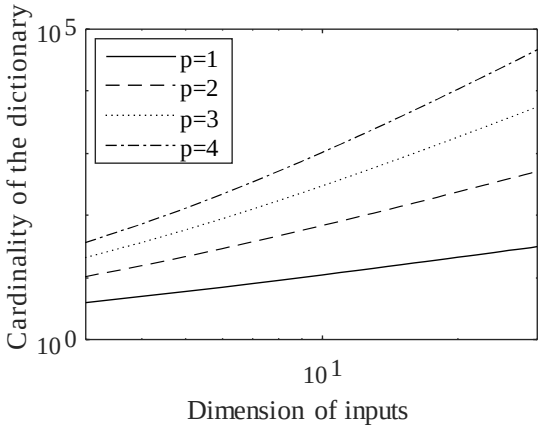


**Figure 13.** Cardinality of the PCE dictionary

To summarize the performance of the investigated surrogate models, the ASPCE stands

out in terms of predictive ability and computational cost. The implemented three speeding-up techniques can effectively reduce the computational cost and ensure the satisfying predictive performance.

*Two-stage multi-criteria global sensitivity analysis and seismic vulnerability*

The PCE based global sensitivity indices of the input parameters with respect to multiple demand parameters are presented in Figure 14, the order of the input is indicated in Table 6, number 17 donates peak ground acceleration (PGA). For all the structural demands, PGA is found to be the most sensitive parameter. Within the bridge parameters, the column height is the most sensitive parameter to column demand. With respect to bearing longitudinal demand, the shear modulus of elastomeric pad has the greatest influence. Apparently, the significant bridge parameters vary from component to component, and the similar observation was reported in [5]. The significant bridge parameters are not consistent for the seismic demands associated with all components. Based on sensitivity indices associated with individual seismic demand, determination of significant bridge parameters to the bridge system is challenging. Using the proposed multi-criteria global sensitivity analysis algorithm, the overall global sensitivity considering multiple structural performance criteria is assessed. Additionally, the different importance of structural performance criteria could be incorporated into the sensitivity analysis process by using weighting factor. The equal importance of all structural performance criteria is used herein. Given different preferences of the structural performance criteria by the decision maker, the sensitivity results can be updated. The uncertainties associated with the weighting factor could also be incorporated in TOPSIS for multi-criteria global sensitivity analysis [48]. The holistic global sensitivity indices of the bridge parameters are computed and presented in Figure 15. The top five most sensitive parameters of bridge input identified by multi-criteria global sensitivity analysis are deck width, span length, shear modulus of elastomeric pad, column height, and concrete compressive strength. The proposed holistic global sensitivity indices aid decision maker to identify the sensitive parameters to the whole bridge system and the ranking of the sensitive parameters can be determined.

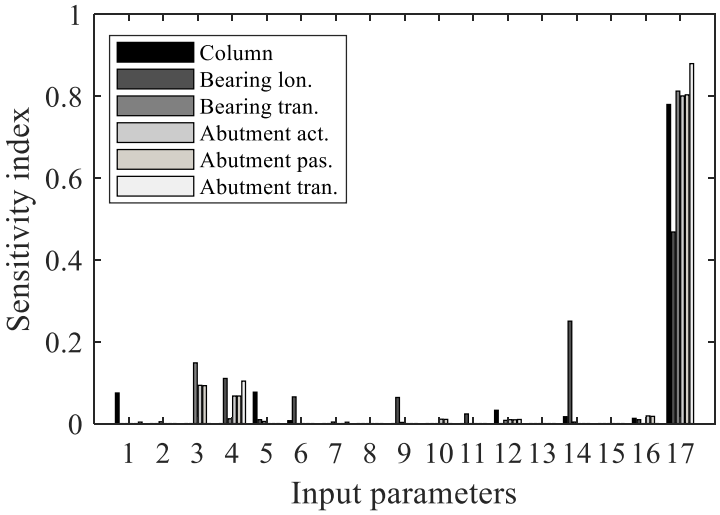


**Figure 14.** Sensitivity indices of the input parameters (Column: column demand; Bearing lon.: bearing longitudinal demand; Bearing tran.: bearing transverse demand; Abutment act: abutment active demand; Abutment pas.: abutment passive demand; and Abutment tran.: abutment transverse demand; the numbers on *x* axis represent different input parameters as indicated in Table 6, number 17 represents PGA)

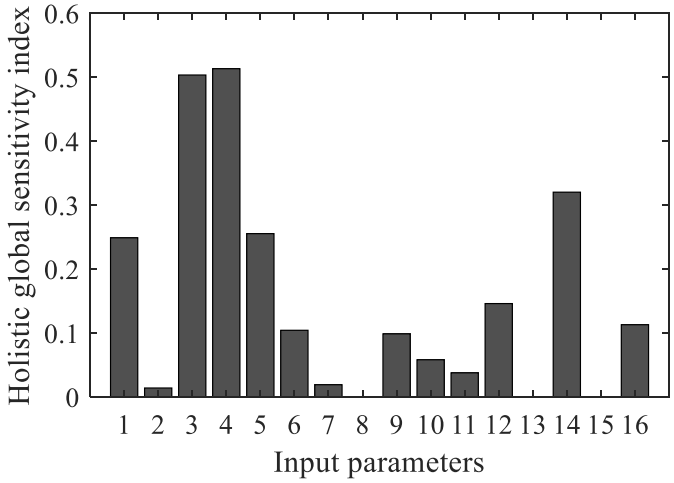


**Figure 15.** Holistic global sensitivity indices (the numbers on *x* axis represent different input parameters as indicated in Table 6)

The multi-dimensional fragility models can be developed using surrogate models in conjunction with logistic regression techniques. A set of input vectors is generated from probabilistic sampling, and the surrogate models are used to compute the demands under the

input vector samples. The set of demands can be computed in seconds using the surrogate models, while the computational cost is large using the original physical models. The same number of probabilistic capacity samples of a component are generated based on probabilistic distributions. Then, a set of Bernoulli binary survive-failure samples is computed by comparing the demand and capacity samples. Finally, the logistic regression is conducted using the survive-failure vectors and the input vectors, and the failure probability for a component is computed as follows [3]

$$PF_{c,IM,ip_1,\dots,ip_k} = \frac{e^{\theta_{c,0}+\theta_{c,IM}ln(IM)+\sum_{j=1}^{k}\theta_{c,j}ln(ip_j)}}{1+e^{\theta_{c,0}+\theta_{c,IM}ln(IM)+\sum_{j=1}^{k}\theta_{c,j}ln(ip_j)}} \quad (29)$$

where $IM$ is seismic intensity measure; $ip_j$ are the prediction input parameters of the structures; and $\theta_{c,j}$ are the regression coefficients.

By computing the structural system level binary survive-failure vector, the structural system level multi-dimensional fragility model can be computed using the same regression technique as

$$PF_{s,IM,ip_1,\dots,ip_k} = \frac{e^{\theta_{s,0}+\theta_{s,IM}ln(IM)+\sum_{j=1}^{k}\theta_{s,j}ln(ip_j)}}{1+e^{\theta_{s,0}+\theta_{s,IM}ln(IM)+\sum_{j=1}^{k}\theta_{s,j}ln(ip_j)}} \quad (30)$$

The multi-dimensional fragility functions can be used to compute failure probabilities for both specific structure and a group of structures. For instance, given the input parameters $ip_j$ for a structure, the structure-specific failure probability can be computed using Eq. (30). Given the probabilistic distributions of input parameters $ip_j$ for a portfolio of structures, the failure probability accounting for the uncertainties can be computed as follows

$$PF_{s,region|IM} = \int\int\dots\int \frac{e^{\theta_{s,0}+\theta_{s,IM}ln(IM)+\sum_{j=1}^{k}\theta_{s,j}ln(ip_j)}}{1+e^{\theta_{s,0}+\theta_{s,IM}ln(IM)+\sum_{j=1}^{k}\theta_{s,j}ln(ip_j)}} f(ip_1)\dots f(ip_k)dip_1\dots dip_k \quad (31)$$

where $f(ip_1)\dots f(ip_k)$ are the PDFs of the input parameters associated with the structures.

To demonstrate the usage and decision making of the proposed holistic sensitivity index, the bridge system fragility curves computed by using different sensitive parameters are

presented in Figure 16. By using the top five holistic sensitive input parameters identified by the proposed approach, the computed fragility is close to the one computed by using all inputs. While by using insensitive parameters identified by the proposed approach (the last five sensitive input parameters), the computed fragility deviates from the one computed by using all inputs. The damage states used in this study are listed in Table 7.

Table 7. Damage states associated with different bridge components [53]

| Component | Slight | | Moderate | | Extensive | | Complete | |
|---|---|---|---|---|---|---|---|---|
| | med. | disp. | med. | disp. | med. | disp. | med. | disp. |
| Concrete Column (curvature ductility) | 1.29 | 0.59 | 2.10 | 0.51 | 3.52 | 0.64 | 5.24 | 0.65 |
| Elastomeric Bearing Fixed-Long (mm) | 28.9 | 0.60 | 104.2 | 0.55 | 136.1 | 0.59 | 186.6 | 0.65 |
| Elastomeric Bearing Fixed-Tran (mm) | 28.8 | 0.79 | 90.9 | 0.68 | 142.2 | 0.73 | 195.0 | 0.66 |
| Abutment-Passive (mm) | 37.0 | 0.46 | 146.0 | 0.46 | N/A | N/A | N/A | N/A |
| Abutment-Active (mm) | 9.8 | 0.70 | 37.9 | 0.90 | 77.2 | 0.85 | N/A | N/A |
| Abutment-Tran (mm) | 9.8 | 0.70 | 37.9 | 0.90 | 77.2 | 0.85 | N/A | N/A |

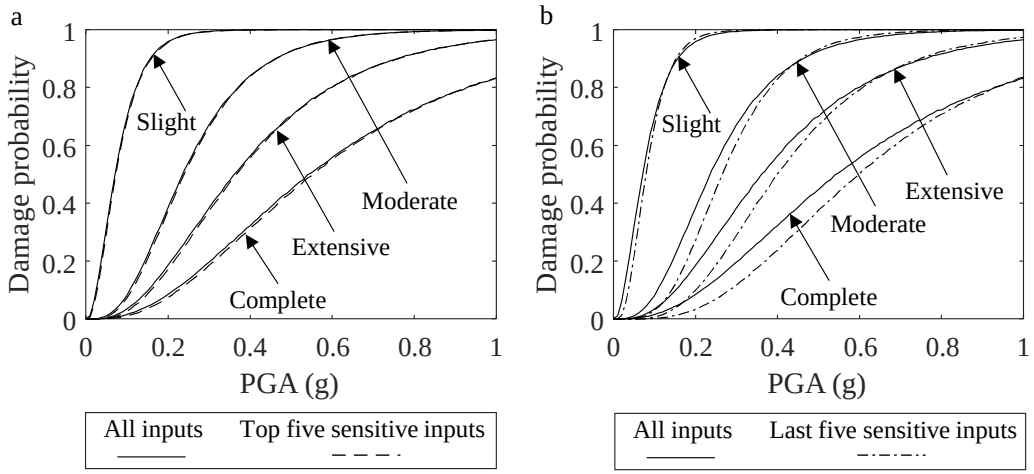


**Figure 16.** Bridge system vulnerability computed using different sensitive parameters for slight, moderate, extensive, and complete damage states

The approach presented in this case reveals the potential application of ASPCE in efficient

regional seismic risk assessment. The road transportation networks usually consist of various bridges. It is necessary to compute the seismic vulnerability of each bridge to assess the regional risk. For the conventional method, developing the fragility curves for all the bridges within a bridge network requires a large number of nonlinear time history analysis, resulting in high computational time. Supposing 100 bridges within a bridge network, if 160 FEM evaluations are required for computing the vulnerability for each bridge, a total number of 16000 FEM evaluations are needed to compute the venerability for all the bridges. The estimated time of computing the vulnerability for all the bridges is 56 days if each FEM evaluation takes 5 minutes. Without surrogate models, the high computational cost hinders the practical application of regional risk assessment. For the sensitivity analysis, a total of $N_{MCS}(M+2) = 10^5 \times (17+2) = 1.9 \times 10^6$ FEM evaluations are required resulting in 6597 days of computational time. In this study, a total of 320 FEM evaluations are used for ASPCE to compute the multidimensional fragility models and global sensitivity, the time of running FEM is only 27 hours. The computational time of seismic vulnerability and global sensitivity analysis for bridge networks can be reduced significantly by using ASPCE.

## 7. Conclusions

This study presents a framework for uncertainty quantification and multi-criteria global sensitivity analysis of structural systems using sparse PCE and acceleration algorithm. Instead of performing the time-consuming greedy algorithms to establish sparse PCE, this study accelerates the computation process in three aspects: probabilistic reduction of basis function candidates; efficient updating using QR decomposition; and implementation of early stopping criterion.

For individual performance criterion, the global sensitivity indices are analytically computed by post-processing the coefficients of PCE model. The significant parameters may not be consistent for all the structural performance criteria, it is difficult to determine the significant parameters considering all the performance criteria. To address this issue, an ASPCE and TOPSIS coupled two-stage multi-criteria global sensitivity analysis algorithm is

proposed. The holistic global sensitivity index is proposed to quantify the overall significance of an input variable considering multiple output parameters.

Two case studies are conducted to illustrate the applicability, accuracy and efficiency of the proposed approach. The approach is verified using MCS through a simple frame structure example. In general, the sparse PCE based methods ASPCE and OMP outperform among the investigated surrogate models for uncertainty quantification, and ASPCE provides accurate estimation of global sensitivity index. Then, the approach is applied on complex bridge structures. The ASPCE and OMP strand out with respect to predictive performance among the five models. The implemented three speeding-up techniques in ASPCE can effectively reduce the computational burden compared with the greedy algorithm OMP. The training time of OMP increases significantly with the total degree of polynomials and input dimensions. In contrast, the training time of ASPCE is independent with input dimension and total degree of polynomials, it can be used for high dimension and high degree problems with reduced computational cost. By using the top five holistic sensitive input parameters identified by the multi-criteria global sensitivity analysis, the computed fragility is close to the one computed by using all inputs. These results demonstrate the applicability and effectiveness of the proposed multi-criteria global sensitivity analysis approach. The presented approaches can aid the uncertainty quantification, multi-criteria global sensitivity analysis, and regional level performance assessment of structural systems in an efficient manner.

**Acknowledgements**

The study has been supported by the National Natural Science Foundation of China (grant no. 51808476) and the Research Grant Council of Hong Kong (project no. PolyU 252161/18E; and PolyU 15219819). The support is gratefully acknowledged. The opinions and conclusions presented in this paper are those of the authors and do not necessarily reflect the views of the sponsoring organizations.

**CRediT author statement**

***Jing QIAN*:** Conceptualization, Investigation, Methodology, Validation, Writing- Original

draft preparation.

***You DONG***: Funding acquisition, Supervision, Investigation, Writing- Reviewing and Editing.

## Appendix A. Example of computation of holistic global sensitivity index

The Sobol' function is expressed as [21]

$$Y_S = \prod_{i=1}^{q} \frac{|4u_i - 2| + a_i}{1 + a_i} \tag{A1}$$

where $u_i$, $i = 1, \ldots, q$ represent input variables, and these input variables follow uniform distribution over [0, 1]; and $a_i$ are nonnegative parameters of the function.

By considering five sets of $a_i$ as listed in Table A.1, five computational functions are obtained.

**Table A.1** Parameters of the output functions

| Output number | $a_1$ | $a_2$ | $a_3$ | $a_4$ |
|---|---|---|---|---|
| 1 | 1 | 5 | 2 | 9 |
| 2 | 15 | 6 | 5 | 8 |
| 3 | 16 | 10 | 5 | 2 |
| 4 | 10 | 2 | 6 | 5 |
| 5 | 12 | 7 | 2 | 5 |

The global sensitivity indices of each input with respect to different outputs are computed and formulated as a sensitivity index matrix as presented in Table A.2.

**Table A.2** Sensitivity index matrix

| Input | Output 1 | Output 2 | Output 3 | Output 4 | Output 5 |
|---|---|---|---|---|---|
| $u_1$ | 0.636 | 0.061 | 0.024 | 0.051 | 0.038 |
| $u_2$ | 0.076 | 0.319 | 0.057 | 0.666 | 0.101 |
| $u_3$ | 0.295 | 0.433 | 0.190 | 0.126 | 0.695 |
| $u_4$ | 0.027 | 0.194 | 0.740 | 0.171 | 0.179 |

The sensitivity ranking of inputs with respect to each output is presented in Table A.3. By

considering different outputs, different sensitivity ranking of inputs can be obtained. Conflicting sensitivity information is obtained, and it is difficult to identify the holistic sensitive parameters by considering all outputs. Compromise decision making should be implemented.

**Table A.3** Sensitivity ranking of inputs with respect to each output

| Input | Output 1 | Output 2 | Output 3 | Output 4 | Output 5 |
|---|---|---|---|---|---|
| $u_1$ | 1 | 4 | 4 | 4 | 4 |
| $u_2$ | 3 | 2 | 3 | 1 | 3 |
| $u_3$ | 2 | 1 | 2 | 3 | 1 |
| $u_4$ | 4 | 3 | 1 | 2 | 2 |

The weighting factors for output 1, output 2, output 3, output 4, and output 5 are considered as 0.6, 0.2, 0.1, 0.05, and 0.05, respectively. By using Eqs. (23) to (28), the holistic global sensitivity indices of each input are computed as presented in Figure A.1. The sensitivity ranking of $u_1$, $u_2$, $u_3$, and $u_4$ considering the trade-off among five outputs can be determined based on holistic global sensitivity index as 1, 3, 2, and 4, respectively.

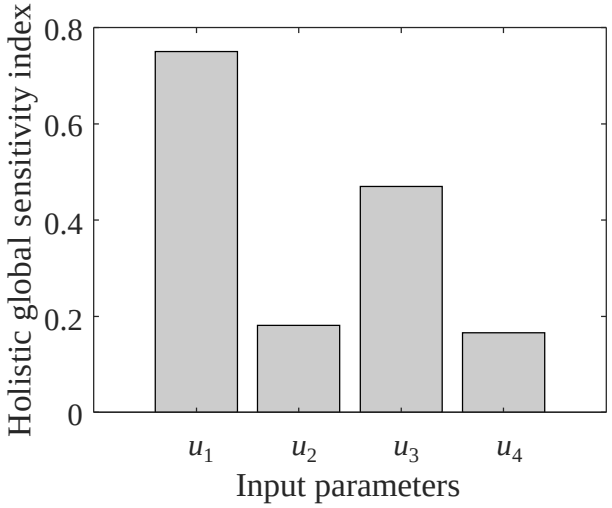


**Figure A.1** Holistic global sensitivity indices of the input parameters

## References

[1] M. Ebad Sichani, J.E. Padgett, Surrogate modelling to enable structural assessment of

collision between vertical concrete dry casks, Struct. Infrastruct. Eng. 15 (2019) 1137–1150. https://doi.org/10.1080/15732479.2019.1618878.

[2] S. Mangalathu, J.S. Jeon, R. DesRoches, Critical uncertainty parameters influencing seismic performance of bridges using Lasso regression, Earthq. Eng. Struct. Dyn. 47 (2018) 784–801. https://doi.org/10.1002/eqe.2991.

[3] J. Ghosh, J.E. Padgett, L. Dueñas-Osorio, Surrogate modeling and failure surface visualization for efficient seismic vulnerability assessment of highway bridges, Probabilistic Eng. Mech. 34 (2013) 189–199. https://doi.org/10.1016/j.probengmech.2013.09.003.

[4] S. Mangalathu, G. Heo, J.S. Jeon, Artificial neural network based multi-dimensional fragility development of skewed concrete bridge classes, Eng. Struct. 162 (2018) 166–176. https://doi.org/10.1016/j.engstruct.2018.01.053.

[5] J.S. Jeon, S. Mangalathu, J. Song, R. Desroches, Parameterized Seismic Fragility Curves for Curved Multi-frame Concrete Box-Girder Bridges Using Bayesian Parameter Estimation, J. Earthq. Eng. 23 (2019) 954–979. https://doi.org/10.1080/13632469.2017.1342291.

[6] X. Guo, D. Dias, C. Carvajal, L. Peyras, P. Breul, Reliability analysis of embankment dam sliding stability using the sparse polynomial chaos expansion, Eng. Struct. 174 (2018) 295–307. https://doi.org/10.1016/j.engstruct.2018.07.053.

[7] M.A. Hariri-Ardebili, B. Sudret, Polynomial chaos expansion for uncertainty quantification of dam engineering problems, Eng. Struct. 203 (2020). https://doi.org/10.1016/j.engstruct.2019.109631.

[8] S.Q. Wu, S.S. Law, Evaluating the response statistics of an uncertain bridge--vehicle system, Mech. Syst. Signal Process. 27 (2012) 576–589.

[9] T. Roncen, J.-J. Sinou, J.P. Lambelin, Non-linear vibrations of a beam with non-ideal boundary conditions and uncertainties--Modeling, numerical simulations and

experiments, Mech. Syst. Signal Process. 110 (2018) 165–179.

[10] N. Wiener, The homogeneous chaos, Am. J. Math. 60 (1938) 897–936.

[11] S. Marelli, B. Sudret, UQLab user manual--Polynomial chaos expansions, Chair Risk, Saf. Uncertain. Quantif. ETH Zürich, 0.9-104 Ed. (2015) 97–110.

[12] G. Blatman, B. Sudret, An adaptive algorithm to build up sparse polynomial chaos expansions for stochastic finite element analysis, Probabilistic Eng. Mech. 25 (2010) 183–197. https://doi.org/10.1016/j.probengmech.2009.10.003.

[13] A. Doostan, H. Owhadi, A non-adapted sparse approximation of PDEs with stochastic inputs, J. Comput. Phys. 230 (2011) 3015–3034. https://doi.org/10.1016/j.jcp.2011.01.002.

[14] G. Blatman, B. Sudret, Adaptive sparse polynomial chaos expansion based on least angle regression, J. Comput. Phys. 230 (2011) 2345–2367. https://doi.org/10.1016/j.jcp.2010.12.021.

[15] E.J. Candès, M.B. Wakin, S.P. Boyd, Enhancing sparsity by reweighted ℓ1 minimization, J. Fourier Anal. Appl. 14 (2008) 877–905. https://doi.org/10.1007/s00041-008-9045-x.

[16] J.D. Jakeman, M.S. Eldred, K. Sargsyan, Enhancing ℓ1-minimization estimates of polynomial chaos expansions using basis selection, J. Comput. Phys. 289 (2015) 18–34. https://doi.org/10.1016/j.jcp.2015.02.025.

[17] J.-J. Sinou, E. Jacquelin, Influence of Polynomial Chaos expansion order on an uncertain asymmetric rotor system response, Mech. Syst. Signal Process. 50 (2015) 718–731.

[18] Y. Dong, D.M. Frangopol, Risk and resilience assessment of bridges under mainshock and aftershocks incorporating uncertainties, Eng. Struct. 83 (2015) 198–208. https://doi.org/10.1016/j.engstruct.2014.10.050.

[19] G.A. Anwar, Y. Dong, C. Zhai, Performance-based probabilistic framework for seismic risk, resilience, and sustainability assessment of reinforced concrete structures, Adv. Struct. Eng. 23 (2020) 1454–1472. https://doi.org/10.1177/1369433219895363.

[20] Y. Li, Y. Dong, D.M. Frangopol, D. Gautam, Long-term resilience and loss assessment of highway bridges under multiple natural hazards, Struct. Infrastruct. Eng. 16 (2020) 626–641. https://doi.org/10.1080/15732479.2019.1699936.

[21] B. Sudret, Global sensitivity analysis using polynomial chaos expansions, Reliab. Eng. Syst. Saf. 93 (2008) 964–979. https://doi.org/10.1016/j.ress.2007.04.002.

[22] A. Saltelli, M. Ratto, T. Andres, F. Campolongo, J. Cariboni, D. Gatelli, M. Saisana, S. Tarantola, Global sensitivity analysis: the primer, John Wiley & Sons, 2008.

[23] H.P. Wan, W.X. Ren, M.D. Todd, Arbitrary polynomial chaos expansion method for uncertainty quantification and global sensitivity analysis in structural dynamics, Mech. Syst. Signal Process. 142 (2020) 106732. https://doi.org/10.1016/j.ymssp.2020.106732.

[24] I.M. Sobol, Global sensitivity indices for nonlinear mathematical models and their Monte Carlo estimates, Math. Comput. Simul. 55 (2001) 271–280. https://doi.org/10.1016/S0378-4754(00)00270-6.

[25] C.-L. Hwang, K. Yoon, Methods for multiple attribute decision making, in: Mult. Attrib. Decis. Mak., Springer, 1981: pp. 58–191.

[26] P. Ni, Y. Xia, J. Li, H. Hao, Using polynomial chaos expansion for uncertainty and sensitivity analysis of bridge structures, Mech. Syst. Signal Process. 119 (2019) 293–311. https://doi.org/10.1016/j.ymssp.2018.09.029.

[27] G. Blatman, B. Sudret, Efficient computation of global sensitivity indices using sparse polynomial chaos expansions, Reliab. Eng. Syst. Saf. 95 (2010) 1216–1229. https://doi.org/10.1016/j.ress.2010.06.015.

[28] G. Georgiou, A. Manan, J.E. Cooper, Modeling composite wing aeroelastic behavior with uncertain damage severity and material properties, Mech. Syst. Signal Process. 32 (2012) 32–43.

[29] S. Salehi, M. Raisee, M.J. Cervantes, A. Nourbakhsh, Efficient uncertainty quantification of stochastic CFD problems using sparse polynomial chaos and compressed sensing, Comput. Fluids. 154 (2017) 296–321. https://doi.org/10.1016/j.compfluid.2017.06.016.

[30] A.J. Smola, B. Schölkopf, Sparse greedy matrix approximation for machine learning, (2000).

[31] J.W. Daniel, W.B. Gragg, L. Kaufman, G.W. Stewart, Reorthogonalization and stable algorithms for updating the Gram-Schmidt ?? factorization, Math. Comput. 30 (1976) 772–795.

[32] R. Baptista, V. Stolbunov, P.B. Nair, Some greedy algorithms for sparse polynomial chaos expansions, J. Comput. Phys. 387 (2019) 303–325. https://doi.org/10.1016/j.jcp.2019.01.035.

[33] G.H. Golub, C.F. Van Loan, Matrix Computations Johns Hopkins University Press, Balt. London. (1996).

[34] P.S. Palar, L.R. Zuhal, K. Shimoyama, T. Tsuchiya, Global sensitivity analysis via multi-fidelity polynomial chaos expansion, Reliab. Eng. Syst. Saf. 170 (2018) 175–190. https://doi.org/10.1016/j.ress.2017.10.013.

[35] G.-H. Tzeng, J.-J. Huang, Multiple attribute decision making: methods and applications, CRC press, 2011.

[36] E. Torre, S. Marelli, P. Embrechts, B. Sudret, A general framework for data-driven uncertainty quantification under complex input dependencies using vine copulas, Probabilistic Eng. Mech. 55 (2019) 1–16. https://doi.org/10.1016/j.probengmech.2018.08.001.

[37] R.B. Nelsen, An Introduction to Copulas. Springer, New York, MR2197664. (2006).

[38] B. Sudret, Y. Caniou, Analysis of covariance (ANCOVA) using polynomial chaos expansions, Safety, Reliab. Risk Life-Cycle Perform. Struct. Infrastructures - Proc. 11th Int. Conf. Struct. Saf. Reliab. ICOSSAR 2013. (2013) 3275–3281. https://doi.org/10.1201/b16387-473.

[39] J.N. Morgan, J.A. Sonquist, Problems in the analysis of survey data, and a proposal, J. Am. Stat. Assoc. 58 (1963) 415–434.

[40] L. Rokach, O.Z. Maimon, Data mining with decision trees: theory and applications, World scientific, 2008.

[41] C.E. Rasmussen, C.K.I. Williams, Gaussian Processes for Machine Learning the MIT Press, Cambridge, Mass. (2006).

[42] B.M. Ayyub, K.-L. Lai, Structural reliability assessment using latin hypercube sampling, in: Struct. Saf. Reliab., 1989: pp. 1177–1184.

[43] Y. Yongfeng, W. Qinyu, W. Yanlin, Q. Weiyang, L. Kuan, Dynamic characteristics of cracked uncertain hollow-shaft, Mech. Syst. Signal Process. 124 (2019) 36–48.

[44] A. Notin, N. Gayton, J.L. Dulong, M. Lemaire, P. Villon, H. Jaffal, RPCM: A strategy to perform reliability analysis using polynomial chaos and resampling: Application to fatigue design, Eur. J. Comput. Mech. 19 (2010) 795–830. https://doi.org/10.3166/ejcm.19.795-830.

[45] S. Tarantola, W. Becker, D. Zeitz, A comparison of two sampling methods for global sensitivity analysis, Comput. Phys. Commun. 183 (2012) 1061–1072.

[46] S. Mangalathu, J.S. Jeon, J.E. Padgett, R. DesRoches, ANCOVA-based grouping of bridge classes for seismic fragility assessment, Eng. Struct. 123 (2016) 379–394. https://doi.org/10.1016/j.engstruct.2016.05.054.

[47] Y. Dong, D.M. Frangopol, D. Saydam, Time-variant sustainability assessment of

seismically vulnerable bridges subjected to multiple hazards, Earthq. Eng. Struct. Dyn. 42 (2013) 1451–1467.

[48] J. Qian, Y. Dong, Multi-criteria decision making for seismic intensity measure selection considering uncertainty, Earthq. Eng. Struct. Dyn. (2020) 1–20. https://doi.org/10.1002/eqe.3280.

[49] Y. Li, Y. Dong, J. Qian, Higher-order analysis of probabilistic long-term loss under nonstationary hazards, Reliab. Eng. Syst. Saf. 203 (2020) 107092. https://doi.org/10.1016/j.ress.2020.107092.

[50] J.W. Baker, T. Lin, S.K. Shahi, N. Jayaram, New ground motion selection procedures and selected motions for the PEER transportation research program, PEER Rep. 3 (2011).

[51] A. Giouvanidis, Y. Dong, Seismic loss and resilience assessment of single-column rocking bridges, Bull. Earthq. Eng. (2020).

[52] Y. Zheng, Y. Dong, Performance-based assessment of bridges with steel-SMA reinforced piers in a life-cycle context by numerical approach, Bull. Earthq. Eng. 17 (2019) 1667–1688.

[53] B.G. Nielson, Analytical fragility curves for highway bridges in moderate seismic zones, Georgia Institute of Technology, 2005.

[54] Y. Xie, Q. Zheng, C.-S.W. Yang, W. Zhang, R. DesRoches, J.E. Padgett, E. Taciroglu, Probabilistic models of abutment backfills for regional seismic assessment of highway bridges in California, Eng. Struct. 180 (2019) 452–467.